J Appl Electrochem (2011) 41:795–801
DOI 10.1007/s10800-011-0297-9

ORIGINAL PAPER

Electrocatalytic activity of $[Ru(bpy)_3]^{2+}$ toward guanine oxidation upon incorporation of surfactants and SWCNTs

Miao-Jing Chen · Xue-Min Weng · Lei-Qing He · Shidang Xu · Hong Li

Received: 23 November 2010 / Accepted: 19 March 2011 / Published online: 20 April 2011

Abstract The homogeneous and mediated oxidation of guanine by $[Ru(bpy)_3]^{2+}$ (2,2′-bipypyridine) in the presence of surfactants and single-walled carbon nanotubes (SWCNTs) has been investigated using cyclic voltammetry, repetitive differential pulse voltammetry and rotating electrode method. In acidic medium, the oxidation of guanine was controlled by mass transport process of $[Ru(bpy)_3]^{2+}$ in solution, leading to a homogeneous electrocatalysis. In neutral medium, the result from emission spectroscopy suggested the formation of the aggregates containing $[Ru(bpy)_3]^{2+}$, dihexadecyl phosphate (DHP) and guanine. The electrocatalysis of $[Ru(bpy)_3]^{2+}$ toward guanine oxidation was promoted by anionic surfactant DHP and, however, hindered by an excess amount of hexadecyl trismethyl ammonium chloride (HTAC) or SWCNTs added to solutions. The electrocatalytic mechanism of $[Ru(bpy)_3]^{2+}$ for guanine oxidation becomes evident, strongly depending on the presence of anionic or cationic surfactants and SWCNTs.

Keywords Guanine · Polypyridyl ruthenium(II) complex · Surfactant · Carbon nanotubes · Electrochemical oxidation

M.-J. Chen · X.-M. Weng · L.-Q. He · S. Xu · H. Li (✉)
Key Laboratory of Electrochemical Technology on Energy Storage and Power Generation of Guangdong Higher Education Institutes, School of Chemistry and Environment, South China Normal University, Guangzhou 510006, People's Republic of China
e-mail: lihong@scnu.edu.cn

1 Introduction

Many considerable efforts have been focused on the oxidation of DNA and its bases because of their important role in the process of mutagenesis and carcinogenesis as well as cancer therapeutics [1, 2]. Guanine is the most easily oxidized bases in DNA and the electrochemical detection of DNA in biological samples is based on the oxidation of guanine [3–5]. It is generally believed that the direct oxidation of guanine at bare electrodes is totally irreversible and suffers from pronounced fouling effects, resulting in poor reproducibility [6, 7]. For this reason, there is an increasing attempt to improve the reproducibility of guanine oxidation using various electrocatalytic approaches [8–10].

Carbon nanotubes (CNTs) on electrode surfaces are used as a promoter to accelerate electron transfer between electro-active species and substrate electrodes [11, 12]. On the other hand, CNTs may be used as a transporter of drug and gene delivery because of their nanoscale dimensions and high-aspect ratio. Therefore, the effects of CNTs both modified on electrode surfaces and added to solutions on the electrode-solution interface become increasingly important. However, poor dispersion of CNTs in both aqueous and nonaqueous solvents has severely limited their effective uses and further development [13, 14]. To adequately disperse CNTs in aqueous solution, various surfactants have been used as dispersants [15–17]. Synchronously, the attachment of surfactants on electrode surfaces can change the interface properties between electrode and solution, subsequently influence the electrocatalytic activities of CNTs and various catalysts [18, 19]. The electron transfer between electroactive species and electrode improved by surfactants was attributed to a synergistic adsorption [20, 21].

Many ruthenium complexes with polypyridyl ligands possess rich electrochemical properties, some of them have been used as electrocatalysts for the oxidation of biomolecules. For example, the electrocatalytic oxidation of purines and DNA by Ru(III) or/and oxo-Ru(IV) complexes has been paid much attention [22–24]. A few homogeneous schemes for guanine oxidation in DNA using $[Ru(bpy)_3]^{2+}$ (2,2′-bipypyridine) as a catalyst were reported by Thorp et al. [25, 26]. Rusling and co-workers demonstrated that there was a direct correlation between the catalytic current and the degree of DNA damage by a series of reports [27, 28]. More recently, based on the fortuitous match between the redox potentials of polypyridyl Ru(III) complexes and DNA, some of them have been used as the mediators for the oxidation of DNA or DNA-wrapped CNTs. Thorp and co-workers showed an electrochemical oxidation of DNA-wrapped CNTs by electrogenerated $[ML_3]^{3+}$ (M = Ru(III), Os(III), and Fe(III); L = 2,2′-bipyridine or 4,4′-dimethyl-2,2′-bipyridine) [29, 30].

In the previous study on the electrocatalytic activity of $[Ru(bpy)_3]^{2+}$ for hypoxanthine (Hx) oxidation in neutral media by rotating electrode methods, the electrocatalytic oxidation of Hx on the rotating Pt electrode conforms to particularly coupled homogeneous reaction, affected by Hx concentration and rotation angular velocity [31]. In this study, the interest is focused on the homogeneous and heterogeneous oxidation of guanine associated with $[Ru(bpy)_3]^{2+}$ in the presence of surfactants and SWCNTs. In acidic medium, the oxidation of guanine upon incorporation of $[Ru(bpy)_3]^{2+}$ on the ITO electrode shows a homogeneous electrocatalysis. In neutral medium, the electrocatalysis of $[Ru(bpy)_3]^{2+}$ toward guanine oxidation is promoted by anionic surfactant DHP and, however, hindered by an excess amount of cationic surfactant HTAC or SWCNTs added to solutions; and then, the authors place emphasis on the electrocatalytic mechanism of $[Ru(bpy)_3]^{2+}$ toward guanine oxidation in the presence of anionic or cationic surfactants and SWCNTs.

2 Experimental

2.1 Chemicals and materials

Tris-hydroxy methyl amino-methane (Tris) from Sigma Chem. Co. was used to prepare buffer solutions. The single-walled carbon nanotubes (SWCNTs) with the inside diameter of 2–5 nm and the length of 10–30 μm were obtained from Chengdu Organic Chemistry Co., Ltd., China. $[Ru(bpy)_3]Cl_2{\cdot}6H_2O$ (Aldrich Chem. Co.), guanine (Shanghai Chem. Co.), dihexadecyl phosphate (DHP) and hexadecyl trismethyl ammonium chloride (HTAC) were used as received. The buffer solution was 10 mmol L^{-1} Tris/50 mmol L^{-1} NaCl of pH 7.2, prepared with double distilled water.

The SWCNTs suspension was prepared by using an appropriate amount of DHP to disperse 3 mg SWCNTs in 5 mL water with the aid of ultrasonic agitation (200 W) for 80 min. And then a desired amount of surfactant-dispersed SWCNT suspensions was mixed with $[Ru(bpy)_3]^{2+}$, DHP and/or guanine with the aid of ultrasonic agitation for 10 min. As shown in Fig. 1, SWCNTs used in this study were effectively dispersed with surfactants and were stable in the test solutions.

2.2 Methods and experimental conditions

Voltammetric measurement was performed on an Autolab PGSTAT-30 electrochemical analysis system with a GPES 4.9 software package (Eco Chemie, The Netherlands) in a regular three-electrode cell of 0.4 mL. Unless otherwise noted, an indium-tin oxide (ITO) was used as the working electrode (20 Ω cm^{-2}, Shenzhen Nanbo Co. Ltd., China), while a platinum sheet was used as counter electrode and a saturated calomel electrode (SCE) as the reference. The ITO surface of 0.72 cm^2 was exposed to the electrolyte solution.

Rotating disk electrode (RDE) and rotating ring-disk electrode (RRDE) experiments were performed in a regular three-compartment cell of 50 mL. A RDE0031 Pt ring–Pt disk (Pt–Pt) electrode matched with Model 636 electrode rotator (Princeton Applied Research, USA) was used. The Pt disk and Pt ring electrodes were molded in polytetrafluoroethylene separately, insulating gap of 0.20 mm between the electrodes. The radius for disk (r_1), inner ring radius (r_2) and outer ring radius (r_3) were 2.26, 2.46, and

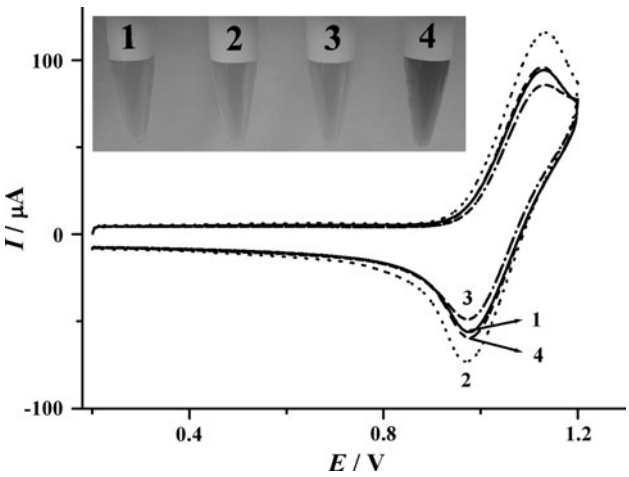

Fig. 1 CVs of 0.25 mmol L^{-1} $[Ru(bpy)_3]^{2+}$ (pH 7.2) in the absence (*1*) and the presence of (*2*) 0.1 mmol L^{-1} DHP (*3*) 0.03 mmol L^{-1} HTAC, (*4*) 0.1 mmol L^{-1} DHP/0.01 g L^{-1} SWCNTs. Scan rate 0.5 V s^{-1}. The *inserted diagram* shows the photographs of test solutions from (1) to (4)

2.69 mm, respectively. The Pt disk ($A_{disk} = 0.160$ cm^2) and Pt ring ($A_{ring} = 0.037$ cm^2) were used as working electrodes. Prior to each experiment, the working electrodes were first polished with 0.5 μm and 0.1 μm alumina pastes on a polishing cloth, respectively; and then, the Pt–Pt electrode was cleaned by ultrasonic agitation in double distilled water for about 10 min and further activated by progressively voltammetric sweeping of 50 cycles at 50 mV s^{-1} scan rate in 0.5 mol L^{-1} H_2SO_4 solution in the potential range from −0.2 to 1.3 V [32]. A Pt flat and a saturated calomel electrode (SCE) were served as counter electrode and reference electrode, respectively.

Steady-state emission spectra were recorded using a RF-2500 spectrofluorimeter. The samples were excited at 450 nm. The luminescence species was immobilized by placing the mixed solutions (30 μL) drop-wise onto the ITO surfaces, and then keeping at a constant temperature of 40 °C for 60 min to evaporate the solvent. The mixed solutions contained 0.2 mmol L^{-1} $[Ru(bpy)_3]^{2+}$, 0.1 mmol L^{-1} guanine and/or 0.1 mmol L^{-1} DHP.

All the measurements were performed at room temperatures (25–27 °C).

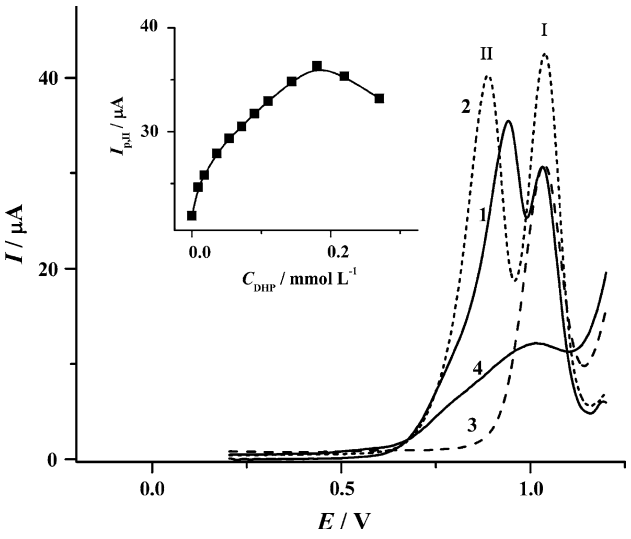

Fig. 2 The first DPVs of 0.1 mmol L^{-1} $[Ru(bpy)_3]^{2+}$/0.10 mmol L^{-1} guanine (pH 7.2) in the presence of DHP (mmol L^{-1}): *1* 0, *2* 0.18. The lines *3* and *4* are the first DPVs of 0.1 mmol L^{-1} $[Ru(bpy)_3]^{2+}$ and 0.10 mmol L^{-1} guanine, respectively. The *inset* shows the relation of oxidative peak II current with DHP concentration

3 Results and discussion

3.1 Electrocatalysis of $[Ru(bpy)_3]^{2+}$ for guanine oxidation tuned by surfactants

Curves 1 and 2 of Fig. 2 is the differential pulse voltammograms (DPVs) of 0.1 mmol L^{-1} $[Ru(bpy)_3]^{2+}$/0.1 mmol L^{-1} guanine in the absence and the presence of 0.18 mmol L^{-1} DHP on the ITO electrode, showing two well-defined oxidative waves (peaks I and II). Compared with the oxidation of $[Ru(bpy)_3]^{2+}$ (curve 3) or guanine (curve 4) alone, the peak I is attributed to Ru(III)/Ru(II) reaction. In the absence of DHP, similar to the previous reports [33], $[Ru(bpy)_3]^{2+}$ can mediate the oxidation of guanine (peak II) as indicated in curve 1 of Fig. 2. The presence of anionic DHP leads to a significant increase of peak II current and a negative shift of peak II potential, revealing that an appropriate amount of DHP facilitates the mediated oxidation of guanine on the ITO electrode (see the inset of Fig. 2). To illustrate the oxidative mechanism of guanine mediated by $[Ru(bpy)_3]^{2+}$ upon incorporation of surfactants, the following factors are analyzed:

3.1.1 Effects of DHP concentration

In the presence of 0.18 mmol L^{-1} DHP, peak II potential negatively shifted to 0.888 V from 0.942 V and peak II current value increased to 37.3 μA from 22.0 μA in contrast to that without DHP. This result suggests that the aggregates containing $[Ru(bpy)_3]^{2+}$, DHP and guanine may be formed and the presence of DHP facilitates the electron transfer between Ru(II)-based aggregates and ITO surface. To further clarify the formation of the aggregates, Fig. 3 shows the emission spectra of $[Ru(bpy)_3]^{2+}$ in the presence of guanine and/or DHP. In the absence of guanine, an intense emission is observed at 572 nm (curve 1), arising from the Ru(II)-to-ligand ($d\pi$–π^*) electron transition [34, 35]. The addition of guanine leads to a decrease in the luminescence with a red-shift of 5 nm in peak position (curve 2), attributed to the association of $[Ru(bpy)_3]^{2+}$ with guanine on the surface by the π–π stacking interaction [36, 37]. When a given mass of DHP was introduced to $[Ru(bpy)_3]^{2+}$ in the presence of DNA, as shown in curve 3 of Fig. 3, the photoluminescence of $[Ru(bpy)_3]^{2+}$ associated with guanine is decreased by DHP. This result is in good agreement with the observations from DPVs in Fig. 2, suggesting the formation of the aggregates containing $[Ru(bpy)_3]^{2+}$, DHP and guanine. The guanine and guanine/DHP in the aggregates may be served as the electron acceptors to influence $[Ru(bpy)_3]^{2+}$-based excited state luminescence [38], leading to a decrease in the emission intensity and a shift in emission peak.

On the other hand, although the peak I potentials do not show a significant shift and the baseline of peak I has a downward adjustment due to the influence of peak II, the peak I current shows an enhancement in the presence of 0.18 mmol L^{-1} DHP (Fig. 2). This may be owed to the influence of DHP on the mass transport process of $[Ru(bpy)_3]^{2+}$, as shown in curves 1 and 2 of Fig. 1,

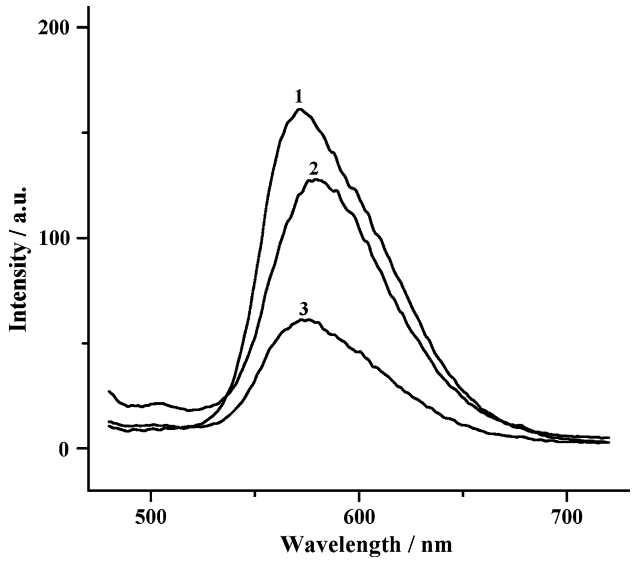

Fig. 3 Emission spectra of $[Ru(bpy)_3]^{2+}$ (*1*), $[Ru(bpy)_3]^{2+}$-guanine (*2*) and $[Ru(bpy)_3]^{2+}$-DHP-guanine (*3*) on the ITO surface (pH 7.2)

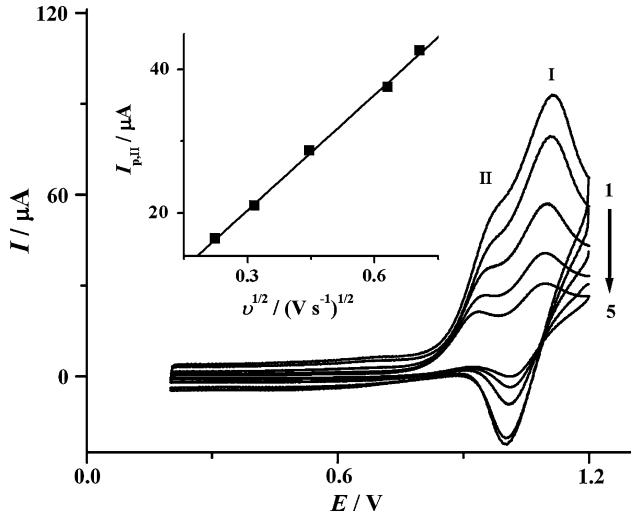

Fig. 4 CVs of 0.1 mmol L^{-1} $[Ru(bpy)_3]^{2+}$/0.10 mmol L^{-1} guanine/0.1 mmol L^{-1} DHP (pH 7.2) at different scan rate (V s^{-1}): *1* 0.50, *2* 0.40, *3* 0.20, *4* 0.10, *5* 0.05. The *inset* shows the relation of oxidative peak II current with the square root of scan rate

the addition of DHP increases redox peak currents of the $[Ru(bpy)_3]^{3+/2+}$ reaction in the absence of guanine. According to the dependence of peak current on the square root of scan rate under mass transport control, the diffusion coefficients of $[Ru(bpy)_3]^{2+}$ in the absence and presence of 0.1 mmol L^{-1} DHP via the Randles-Sevčik equation are 5.88×10^{-6} cm^2 s^{-1} and 7.84×10^{-6} cm^2 s^{-1}, respectively [32]. The result suggests that the association of $[Ru(bpy)_3]^{2+}$ with DHP facilitates its mass transport in electrolyte solution.

3.1.2 *Effects of scan rate and voltammetric sweeping number*

In the presence of $[Ru(bpy)_3]^{2+}$ and DHP, as depicted by Fig. 4, the peak II reaction only exhibits an oxidative wave on the forward curve and no reductive wave is observed on the reversal sweeping. This result is similar to the oxidation of guanine on various solid electrodes, showing an irreversible process due to the strong adsorption of 8-oxo-guanine product [7, 39]. With increasing scan rate, the peak II is shifted to a more positive potential and shows a linear relation with the square root of scan rate (see the inset of Fig. 4). Furthermore, when the voltammetric sweeping number increases, as shown in Fig. 5, the peak II exhibits a continuous decrease, suggesting that the 8-oxo-guanine product hinders the mediated oxidation of guanine by $[Ru(bpy)_3]^{2+}$ in the presence of DHP. However, under the experimental conditions, the ITO surface suffers from less fouling effects than that as reported previously [6, 7], and the oxidized products of guanine hardly depress the redox reaction of peak I.

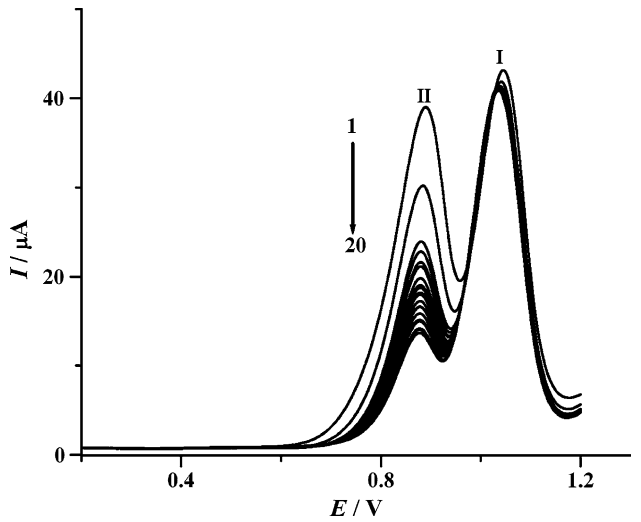

Fig. 5 Progressive DPVs of 0.10 mmol L^{-1} $[Ru(bpy)_3]^{2+}$/0.10 mmol L^{-1} guanine/0.1 mmol L^{-1} DHP (pH 7.2)

3.1.3 *Rotating ring-disk electrode measurement*

When rotating Pt disk electrodes displace the static ITO electrode, as shown in Fig. 6, an increase in the rotating speed facilitates the mass transport of Ru(II)-based species. Under mass-transport controlled conditions for the oxidation of guanine in the presence of 0.1 mmol L^{-1} DHP, the dependence of limiting current plateau on the square root of rotation rate conforms to the Levich equation as depicted by the inset of Fig. 6 [32]. However, when the DHP concentration is less than 0.04 mmol L^{-1}, no limiting current plateau is observed, which is displaced by an oxidative peak as shown in Fig. 7. This result reveals that

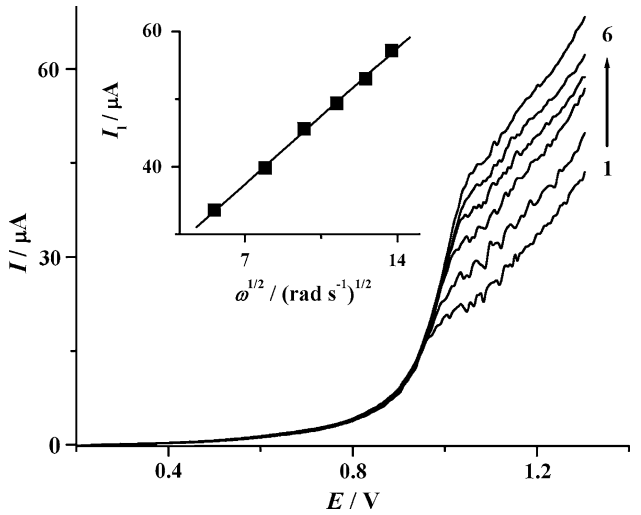

Fig. 6 Voltammetric curves of 0.2 mmol L^{-1} $[Ru(bpy)_3]^{2+}$/ 0.1 mmol L^{-1} guanine/0.1 mmol L^{-1} DHP (pH 7.2) on the Pt disk electrode at different rotating rates (r s^{-1}): *1* 5, *2* 10, *3* 15, *4* 20, *5* 25, *6* 30. Scan rate: 5 mV s^{-1}, ring potential: 0.3 V. The *inset* shows the relation of limiting plateau current at 1.2 V with the square root of rotation speed

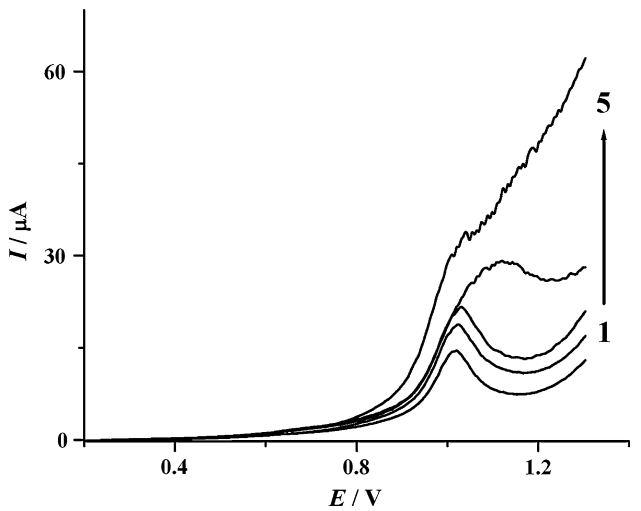

Fig. 7 Voltammetric curves of 0.2 mmol L^{-1} $[Ru(bpy)_3]^{2+}$/ 0.1 mmol L^{-1} guanine (pH 7.2) on rotating Pt disk electrode with 15 r s^{-1} at different DHP concentrations (mmol L^{-1}): *1* 0, *2* 0.005, *3* 0.01, *4* 0.04, *5* 0.08. Scan rate 5 mV s^{-1}

the addition of DHP facilitates the charge transfer between the aggregates and electrode as well as the mass transport process. Of course, with increasing the guanine concentration, the limiting current plateau is transformed into an oxidative peak due to an elimination of concentration polarization in Fig. 8(a). Synchronously, when the ring potential is held at 0.3 V, a well-defined current plateau is observed at low guanine concentrations, suggesting that an excess amount of $[Ru(bpy)_3]^{3+}$ is reduced on the Pt ring electrode, originated from the oxidative product of Pt

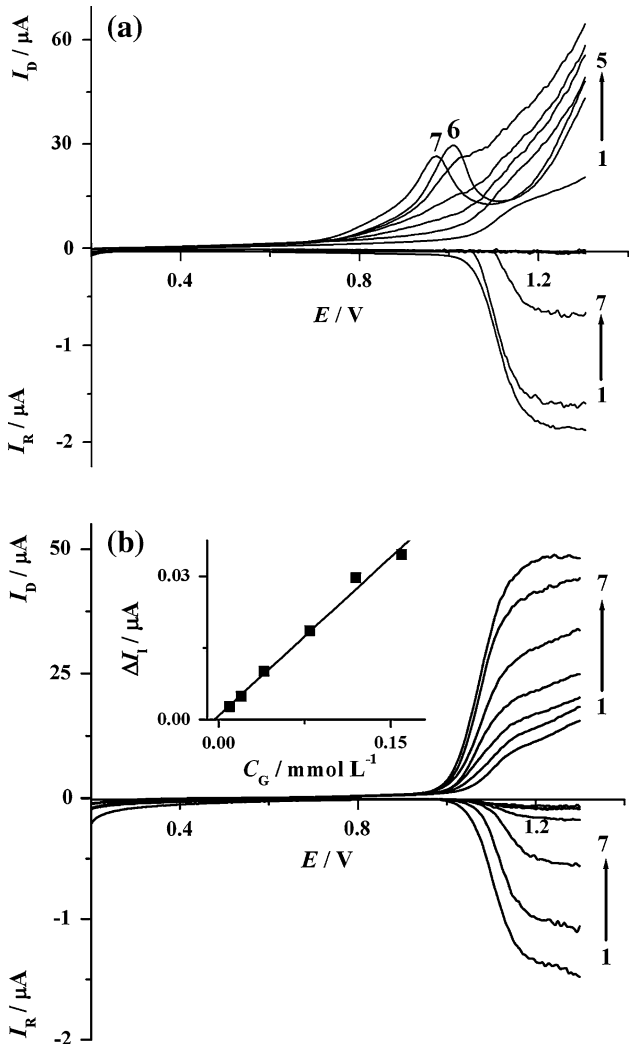

Fig. 8 Voltammetric curves of 0.2 mmol L^{-1} $[Ru(bpy)_3]^{2+}$ on rotating Pt–Pt electrode with15 r s^{-1} rotation rate at different guanine concentrations (mmol L^{-1}) with pH values of 7.2 (**a**) or 3.0 (**b**): *1* 0, *2* 0.01, *3* 0.02, *4* 0.04, *5* 0.08, *6* 0.12, *7* 0.16. Scan rate: 5 mV s^{-1}. Ring potential: 0.3 V. The *inset* shows the relation of limiting plateau current at 1.25 V (plot b) with guanine concentration

disk electrode. At high-guanine concentration, no significant ring current is observed due to the complete consumption of $[Ru(bpy)_3]^{3+}$.

When the neutral medium is adjusted to an acidic medium, the height of disk current plateau is linear with the guanine concentration in the range up to 0.16 mmol L^{-1} as shown in Fig. 8(b), and the relative coefficient is 0.99. These results imply that voltammetric measurement on the rotating Pt electrode may be developed to monitor guanine concentration changes catalyzed by $[Ru(bpy)_3]^{2+}$ reaction. In acidic medium, the oxidation of guanine in the presence of $[Ru(bpy)_3]^{2+}$ conforms to the homogeneous electrocatalysis, i.e., $[Ru(bpy)_3]^{3+}$ generated from the oxidative product of $[Ru(bpy)_3]^{2+}$ on the disk electrode is coupled with a homogeneous reaction of guanine.

3.1.4 *Effects of cationic surfactant HTAC*

When anionic DHP is substituted by cationic surfactants such as HTAC, Fig. 9 reveals that an excess amount of HTAC depresses the redox reactions of $[Ru(bpy)_3]^{2+}$ and the mediated oxidation of guanine, so the current values of peaks I and II exhibit a decrease with the rise of HTAC concentration. In the presence of 0.07 mmol L^{-1} HTAC, peak I even disappeared and peak II potential shifted to 1.020 V from 0.961 V. This result suggests that HTAC is hardly served as bridging molecules to associate with the mediated oxidation of guanine by $[Ru(bpy)_3]^{2+}$ based on the electrostatic repulsion between cationic HTAC and $[Ru(bpy)_3]^{2+}$. Furthermore, the adsorption of surfactants on the ITO electrode may hinder the redox reaction of positively charged $[Ru(bpy)_3]^{2+}$ as shown in the curve 3 of Fig. 1, as a result, high-HTAC concentration blocks the redox reactions of $[Ru(bpy)_3]^{2+}$ and the mediated oxidation of guanine.

To sum up the above discussion, in neutral medium in the presence of DHPA (DHP anion), the mediated mechanism of guanine (G) by $[Ru(bpy)_3]^{2+}$, denoted as Ru(II), is proposed as follows:

$$Ru(II) + 2DHPA + G \rightleftharpoons \{Ru(II) - DHPA_2 - G\} \quad (1)$$

$$\{Ru(II) - DHPA_2 - G\} - e \underset{ITO}{\rightleftharpoons} \{Ru(III) - DHPA_2 - G\} \quad (2)$$

$$\{Ru(III) - DHPA_2 - G\} \rightleftharpoons \{Ru(II) - DHPA_2 - G_{Ox}\} \quad (3)$$

$$\{Ru(II) - DHPA_2 - G_{Ox}\} \rightleftharpoons Ru(II) + 2DHPA + G_{Ox} \quad (4)$$

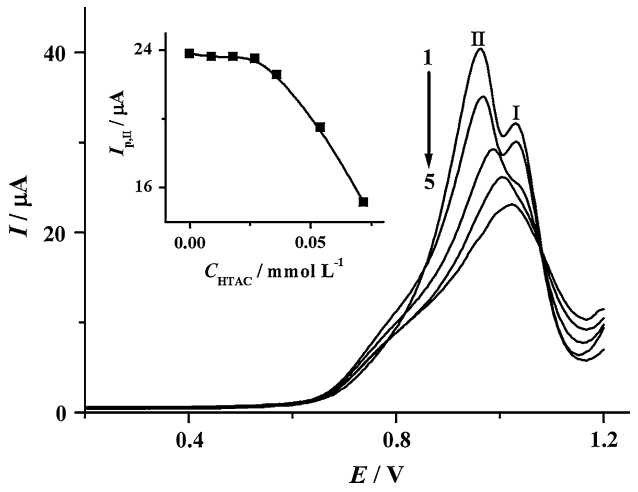

Fig. 9 The first DPVs of 0.10 mmol L^{-1} $[Ru(bpy)_3]^{2+}$/0.10 mmol L^{-1} guanine (pH 7.2) at different concentrations of HTAC (mmol L^{-1}): *1* 0.01, *2* 0.03, *3* 0.04, *4* 0.05, *5* 0.07. The *inset* shows the relation of oxidative peak II current with HTAC concentration

3.2 Electrocatalysis of $[Ru(bpy)_3]^{2+}$ for guanine oxidation tuned by DHP-SWCNTs

The results mentioned above show that the presence of DHP promotes the mediated oxidation of guanine by $[Ru(bpy)_3]^{2+}$ in neutral medium. It is now interesting to investigate whether the oxidation of guanine could be influenced by single-walled carbon nanotubes (SWCNTs) dispersed with DHP. For this reason, DHP-SWCNTs displaces DHP to conduct the corresponding examination, the result is shown in Fig. 10. When the SWCNTs concentration is fixed at 20 mg L^{-1} (curve 1), the increasing concentration of DHP can promote the mediated oxidation of guanine, as a result, the peak II current increases with the rise of DHP concentration (see the inset of Fig. 10). However, while the SWCNTs concentration is decreased to 10 and 5 mg L^{-1} (curves 2 and 3), respectively, the current values of peaks I and II shows an increase compared with that in the presence of 20 mg L^{-1} SWCNTs. In addition, the current responses of peaks I and II at these SWCNTs concentrations, are smaller than that in the absence of SWCNTs (curve 4). This result suggests that the presence of SWCNTs may weaken the mass transport process of Ru(II)-based species in electrolyte solution due to the association of Ru(II)-$DHPA_2$-G aggregates with SWCNTs. Of course, in the absence of guanine, the addition of SWCNTs also weakens the mass transport of $[Ru(bpy)_3]^{2+}$, the curve 4 in Fig. 1 exhibits a smaller current in comparison to the case without SWCNTs. These results provide

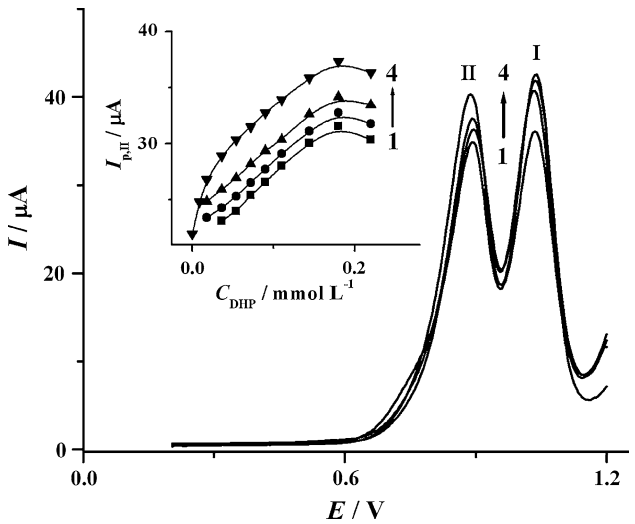

Fig. 10 The first DPVs of 0.10 mmol L^{-1} $[Ru(bpy)_3]^{2+}$/0.10 mmol L^{-1} guanine/0.1 mmol L^{-1} DHP (pH 7.2) in the presence of SWCNTs (g L^{-1}): *1* 0.02, *2* 0.01, *3* 0.005, *4* 0. The *inset* shows the relation of oxidative peak II currents as a function of DHP concentration in the absence (*inverted dark triangle*) and presence of 0.005 (*dark triangle*), 0.01 (*dark circle*) or 0.02 (*dark square*) g L^{-1} SWCNTs

a significant foundation for monitoring the delivery of drugs and biomolecules using CNTs as a transporter.

4 Conclusions

The electrocatalytic kinetics of $[Ru(bpy)_3]^{2+}$ for guanine oxidation strongly depends on the presence of anionic or cationic surfactants and SWCNTs. In acidic medium, the electrocatalytic process of $[Ru(bpy)_3]^{2+}$ toward guanine oxidation is under a diffusion control and corresponds to a homogeneous electrocatalysis. In neutral medium, the electrocatalysis of $[Ru(bpy)_3]^{2+}$ for guanine oxidation is promoted by anionic DHP and, however, hindered by an excess amount of cationic HTAC or SWCNTs added to solutions. The electrocatalytic mechanism of $[Ru(bpy)_3]^{2+}$ is proposed.

Acknowledgments The authors are grateful to the Specialized Research Fund for the Doctoral Program of Higher Education of China (No. 20094407120008) for their financial support.

References

1. Kanvah S, Joseph J, Schuster GB et al (2010) Acc Chem Res 43:280
2. Knutson CG, Rubinson EH, Akingbade D et al (2009) Biochemistry 48:800
3. Drummond TG, Hill MG, Barton JK (2003) Nat Biotechnol 21:1192
4. Gooding JJ (2002) Electroanalysis 14:1149
5. Voityuk AA, Jortner J, Bixon M et al (2000) Chem Phys Lett 324:430
6. Sun W, Li YZ, Duan YY et al (2008) Biosens Bioelectron 24:988
7. Ferapontova EE (2004) Electrochim Acta 49:1751
8. Abbaspour A, Mehrgardi MA (2004) Anal Chem 76:5690
9. Hong W, Li H, Yao S et al (2009) Electrochim Acta 54:3250
10. Gao ZQ (2007) Sens Actuators B 123:293
11. Valcárcel M, Cárdenas S, Simonet BM (2007) Anal Chem 79:4788
12. Li J, Ng HT, Cassell A et al (2003) Nano Lett 3:597
13. Sinani VA, Gheith MK, Yaroslavov AA et al (2005) J Am Chem Soc 127:3463
14. Maeda Y, Kimura S, Hirashima Y et al (2004) J Phys Chem B 108:18395
15. Erdem A, Papakonstantiou P, Murphy H (2006) Anal Chem 78:6656
16. Krause B, Mende M, Pötschke P et al (2010) Carbon 48:2746
17. Rastogi R, Kaushal R, Tripathi SK et al (2008) J Colloid Interface Sci 328:421
18. Sakthivel M, Schlange A, Kunz U et al (2010) J Power Source 195:7083
19. Sanghavi BJ, Srivastava AK (2010) Electrochim Acta 55:8638
20. Rusling JF (1997) Colloids Surf A 123–124:81
21. Mackay RA (1994) Colloids Surf A 82:1
22. Szalai VA, Thorp HH (2000) J Phys Chem B 104:6851
23. Tan CP, Liu J, Chen LM et al (2008) J Inorg Biochem 102:1644
24. Arkin MR, Stemp EDA, Pulver SC et al (1997) Chem Biol 4:389
25. Johnston DH, Thorp HH (1996) J Phys Chem 100:13837
26. Armistead PM, Thorp HH (2001) Anal Chem 73:558
27. Zhou LP, Rusling JF (2001) Anal Chem 73:4780
28. Mugweru A, Rusling JF (2002) Anal Chem 74:4044
29. Napier ME, Hull DO, Thorp HH (2005) J Am Chem Soc 127:11952
30. Campbell FJ, Napier ME, Feldberg SW et al (2010) J Phys Chem B 114:8861
31. Yan XX, Li H, Xu ZH et al (2009) Bioelectrochemistry 74:310
32. Bard AJ, Faulkner LR (1980) Electrochem Method. Wiley, NewYork
33. Lim SH, Wei J, Lin JY (2004) Chem Phys Lett 400:578
34. Zou XH, Li H, Yang G et al (2001) Inorg Chem 40:7091
35. Shao JY, Sun T, Ji SB et al (2010) Chem Phys Lett 492:170
36. Atsumi M, González L, Daniel C (2007) J Photochem Photobiol A 190:310
37. Liu SY, He YB, Chan WH et al (2006) Tetrahedron 62:11687
38. Johansson E, Zink JI (2007) J Am Chem Soc 129:14437
39. Oliveira-Brett AM, Diculescu V, Piedade JAP (2002) Bioelectrochemistry 55:61